Photophysics of novel 22π porphyrinoids

Daniel O. Mártire[a,b]**, Sigrid Russell**[a]**, Hans-Jürgen Dietrich**[c†]**, Carlos J. Cobos**[b] **and Silvia E. Braslavsky***[a]

[a] *Max-Planck-Institut für Bioanorganische Chemie (formerly für Strahlenchemie), Postfach 10 13 65, D-45413 Mülheim an der Ruhr, Germany*
[b] *Instituto de Investigaciones Fisicoquímicas Teóricas y Aplicadas (INIFTA), CCT-La Plata-CONICET, Universidad Nacional de La Plata, La Plata, Argentina*
[c] *Institut für Organische Chemie, Universität Köln, Greinstrasse 4, D-50939 Köln, Germany*

Dedicated to Professor Emanuel Vogel in memoriam

ABSTRACT: The photophysical properties of toluene solutions of two new 22π expanded porphycene compounds were measured using a combination of various steady-state and time-resolved techniques. The determined triplet energy ($E_T = 109 \pm 3$) kJ.mol^{-1}, coincident with the calculated $E_T = (96.0 \pm 10)$ kJ.mol^{-1}, of both red absorbing compounds is higher than the energy required to excite ground state molecular oxygen to singlet molecular oxygen. However, the intersystem crossing yield is very low (*ca.* 10^{-2}), which makes these compounds poor photosensitizers. The triplet state yield of the two expanded 22π porphyrinoid compounds is much lower than that of the parent porphycene, whereas their fluorescence is as high (*ca.* 30%) as the value for porphycene. The slower than diffusional quenching rate constant of a porphycene triplet state by the two new compounds reflects a steric hindering factor of the exothermic energy transfer.

KEYWORDS: porphycenes, porphyrins, singlet molecular oxygen, near-infrared emission, sensitizers.

INTRODUCTION

A first example of expansion of the 18π porphycene (**1**), an isomer of porphyrin [1], to the 22π homologous class of the acetylene-cumulene porphyrinoid parent **3** has been achieved by synthesis of **4** [2–4] and the tetrahydro- derivative **6** (Scheme 1) [5]. The alternatively expanded structure of type **5** has not been accessible so far. However, a synthetic approach different from the method employed for the acetylene-cumulene compounds afforded the expanded porphycenes **7** and **8**, which in terms of 22π electronic structure relate to **5** as **6** relates to **3** [6].

An investigation of the photophysical properties is of interest for several reasons: on the one hand, porphycenes

are considered candidates for use as second-generation sensitizers in photodynamic therapy, which includes their capacity to generate singlet molecular oxygen, O$_2$($^1\Delta_g$), by *in vivo* sensitization [7]. The expanded compounds **4** and **6** have been found to differ considerably in their photophysical properties, such as fluorescence and triplet yields and energies, from those of the parent porphycenes (**1**, **2**) [8, 9]. This is in line with the properties of other red-absorbing porphyrinoid systems possessing (4n + 2) conjugated π electrons (with n ≥ 5). For example, the triplet energies of other expanded 22π and 26π porphycenes [8], phthalocyanines [10], and naphthalocyanines [11] are close to or even lower than the energy (94.4 kJ.mol^{-1}) [12] required to promote ground-state oxygen, O$_2$($^3\Sigma_g^-$), to O$_2$($^1\Delta_g$).

On the other hand, measurements of the photophysical properties of such compounds are often not trivial in view of the difficulty associated with the availability of appropriate references in the far-red spectral region. The lack of phosphorescence of the 22π and 26π porphycenes

---

*Correspondence to: Silvia E. Braslavsky, email: braslavskys@mpi-muelheim.mpg.de, fax: +49 (208)-306-3951

†Current address: BASF IT Services GmbH, Ludwigshafen, Germany
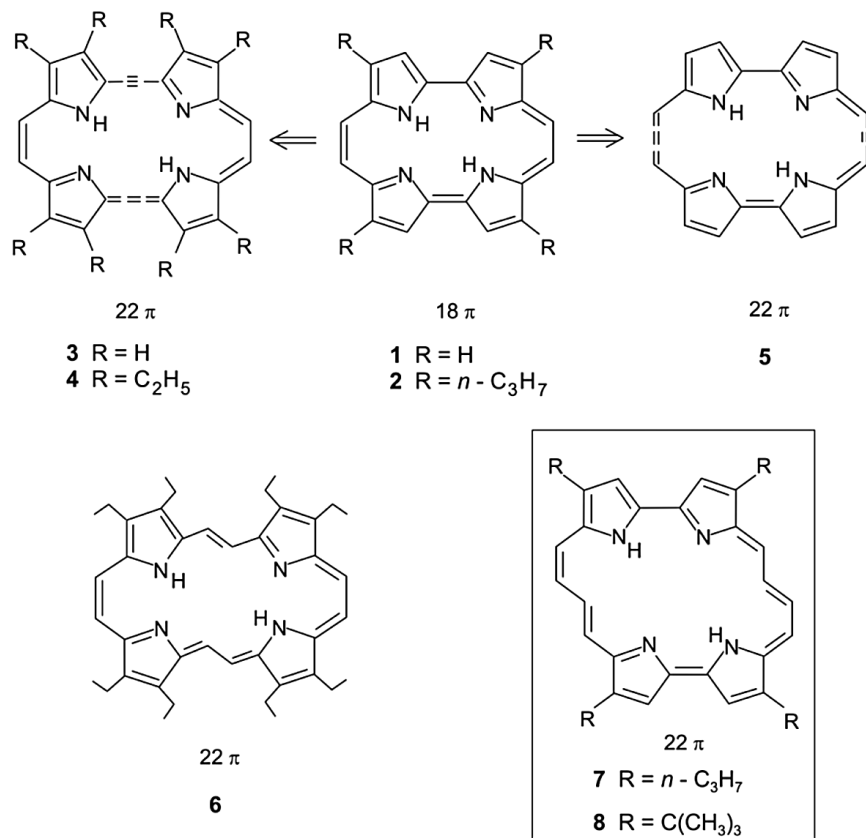
Scheme 1. Formal expansion of Porphycene (**1**) by acetylene-cumulene structural units to 22π homologs **3** (Type I) and **5** (Type II), the Type I derivatives **4** and **6** studied previously,[8] and the Type II-related compounds **7** and **8** under study in this report

at room temperature in normal solvents demands, furthermore, a judicious choice of the methods for triplet energy determination.

The time-dependent density functional theory (TD-DFT) calculations of the T-T absorption spectrum of compound **7** delivered data in good agreement with those experimentally determined.

RESULTS

The absorption spectra of **7** (Fig. 1) and **8** are very similar. The maxima in nm (molar absorption coefficients, ε/M^{-1}.cm^{-1}) are for compound **7**: 385 (shoulder, $\varepsilon = 30$ 700), 445 ($\varepsilon = 179$ 700), 560 (shoulder, $\varepsilon = 4$ 800), 653 ($\varepsilon = 28$ 900), 728 ($\varepsilon = 9$ 000), and 817 ($\varepsilon = 43$ 700); for compound **8**: 388 (shoulder, $\varepsilon = 29$ 900), 446 ($\varepsilon = 186$ 200), 563 (shoulder, $\varepsilon = 5$ 100), 652 ($\varepsilon = 35$ 900), 729 ($\varepsilon = 8$ 100), and 821 ($\varepsilon = 39$ 000).

Upon irradiation, some permanent bleaching of both compounds (**7** and **8**) was observed, especially in the red flank of the absorption band. The quantum yield of this bleaching was estimated to be *ca.* 10^{-2}.

Singlet state properties

The fluorescence spectra of the two porphyrinoids, **7** (Fig. 1) and **8** (not shown), fully overlap but show some
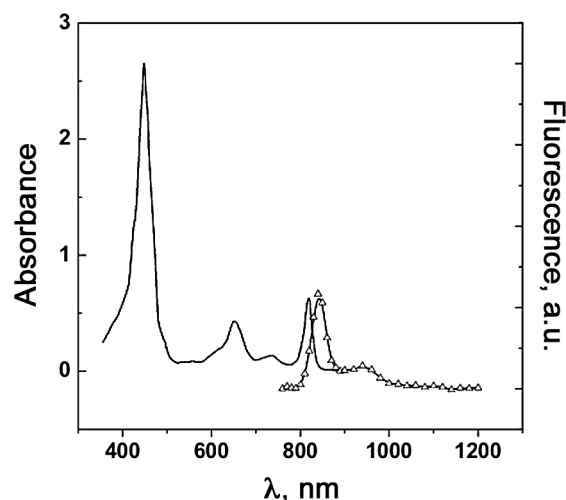

Fig. 1. Absorption spectrum of **7** (solid line) and Q-band-normalized uncorrected fluorescence spectrum of an air-saturated solution of **7** (Δ). For the fluorescence spectrum $A_{651} = 0.171 \pm 0.001$, $\lambda^{exc} = 651$ nm. The fluorescence spectrum of a matched-absorbance solution of **8** was identical, but slightly less intense (see Table 1)

difference in intensity (*vide infra*). The fluorescence spectra are a relatively good mirror image of the respective lowest energy Q-band with a second maximum imaging the second lowest Q-band (probably a vibrational band).

Table 1. Photophysical properties of **7** and **8** in toluene at room temperature

	7	**8**
E_S /(kJ.mol^{-1}) [a]	146 ± 8	146 ± 8
τ_S /ns [b]	2.0	1.9
Φ_f [c]	0.30 ± 0.05	0.25 ± 0.05
Φ_{ic}^{0} [d,e]	0.72 ± 0.07	0.77 ± 0.07
τ_T /μs [f]	77 ± 8	36 ± 4
Φ_T^{0} [e]	$(2.5 \pm 0.9) \times 10^{-2}$	$(1.5 \pm 0.6) \times 10^{-2}$
E_T /(kJ.mol^{-1}) [g]	$106.4 \leq E_T \leq 112$	$106.4 \leq E_T \leq 112$
$\Delta\varepsilon(500)$	$(1.0 \pm 0.4) \times 10^{4}$	$(1.2 \pm 0.5) \times 10^{4}$
Φ_Δ [h]	$< 10^{-3}$	$< 10^{-3}$

[a]Calculated from the fluorescence maximum in toluene. [b]Measured in air-saturated solutions. [c]See text for the calculation from LIOAS data. [d]Calculated from LIOAS data and $[E^{exc} \times (\alpha - 1) + E_S] \times E_S^{-1}$. [e]Superscript 0 indicates the absence of oxygen. [f]T-T spectrum measured in degassed solutions at $\lambda^{exc} = 650$ nm. [g]See text for estimates of limits and for TD-DFT calculations. [h]$O_2(^1\Delta_g)$ not detected.

The Stokes shift is relatively large, most likely reflecting the flexibility of the large macrocycle (Fig. 1).

Since the absorbances of the sample solutions used for the fluorescence spectra had been matched at the excitation wavelength, the ratio of the non-normalized spectral areas is equal to the ratio of the fluorescence quantum yields, Φ_f; hence $\Phi_f(\mathbf{7})/\Phi_f(\mathbf{8}) = 1.21$. For the fluorescence lifetimes, τ_S, see Table 1.

Triplet state properties

Neither **7** nor **8** exhibit any phosphorescence. Their measured T-T absorption spectra immediately after the laser pulse (ΔA_0 vs. λ) are shown in Fig. 2. The calculated T1 to T2 absorption coefficients are shown in Fig. 3. The agreement between both sets is good (within the respective errors).

The triplet states of **7** and **8** decayed monoexponentially both in the presence and absence of oxygen (see, e.g., Inset in Fig. 2). Their lifetimes in degassed toluene solution were (77 ± 8) and (36 ± 4) μs, respectively. Oxygen led not only to quenching of the triplets but also to enhanced S → T intersystem crossing, as did the addition of 1-iodopropane (a heavy atom effect). An increase in ΔA_0 resulted in each case, as illustrated in Figs 4a and 4b for **8** (the similar effects of oxygen and 1-iodopropane on **7** are not shown). Linear Stern-Volmer plots of $1/\tau_T$ vs $[O_2]$ in toluene (not shown) yielded the corresponding quenching constants: $k_q^{O2} = (4.1 \pm 0.2) \times 10^8$ and $(2.5 \pm 0.2) \times 10^8$ M^{-1}.s^{-1} for triplet **7** and **8**, respectively. For triplet **8** in 1-iodopropane, $k_q^{O2} = (2.6 \pm 0.6) \times 10^8$ M^{-1}.s^{-1}.

The zero time absorbances at the wavelength of the T-T absorption maxima of **2** (reference), **7** and **8**, ΔA_0, were linear functions of the laser pulse fluence, E_L. Using the literature data for **2** (vide supra) and the comparative method [13] the slopes of the straight lines in Fig. 5
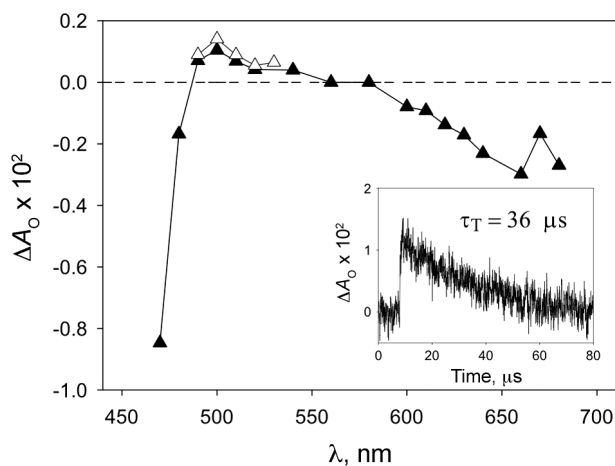

Fig. 2. T-T absorption spectra of (Δ) **7** and (▲) **8** immediately after the laser pulse at $\lambda^{exc} = 650$ nm in degassed toluene solutions. Inset: Triplet state decay for **8** in degassed toluene, $\lambda^{obs} = 500$ nm
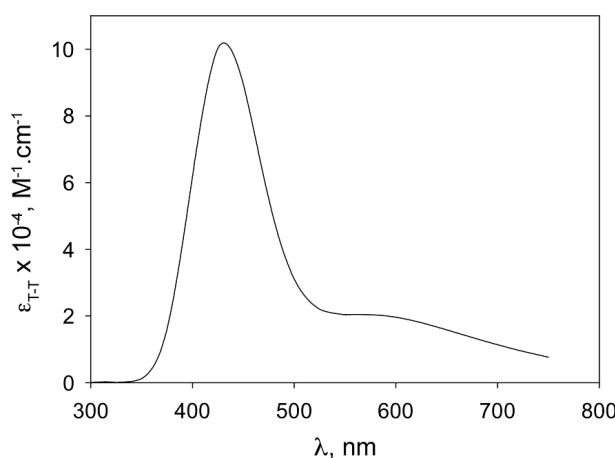

Fig. 3. Calculated values of $\Delta\varepsilon_{T\text{-}T}$ for compound **7**

afforded values of the product $[\Delta\varepsilon(500) \times \Phi_T^0] = (259 \pm 96)$ and (193 ± 73) M^{-1}.cm^{-1} for **7** and **8**, respectively.

The $\Delta\varepsilon(500)$ values for the triplet states of **7** and **8** were determined from comparative measurements of the transient absorbance increase at 500 nm (absorbance of the triplet state) and decrease at 470 nm. At the latter wavelength the triplet states are assumed not to absorb (we are aware of the fact that this is a not-so-good assumption) and only ground state depletion is considered (cf. Fig. 2).

The ratio of the slopes of the linear plots of ΔA_0 for **7** and **8** vs E_L at λ^{obs} 470 and 500 nm afforded $\Delta\varepsilon(500) = (1.0 \pm 0.4) \times 10^4$ M^{-1}.cm^{-1} for **7** and $\Delta\varepsilon(500) = (1.2 \pm 0.5) \times 10^4$ M^{-1}.cm^{-1} for **8**, which together with the product $[\Delta\varepsilon(500) \times \Phi_T^0]$ (vide supra) yielded $\Phi_T^0 = (0.025 \pm 0.009)$ for **7** and (0.015 ± 0.006) for **8**.

In the LIOAS experiments, the amplitude (H) of the first signal deflection is related to the laser fluence (E_L) and to A by Equation (1) [14–16],

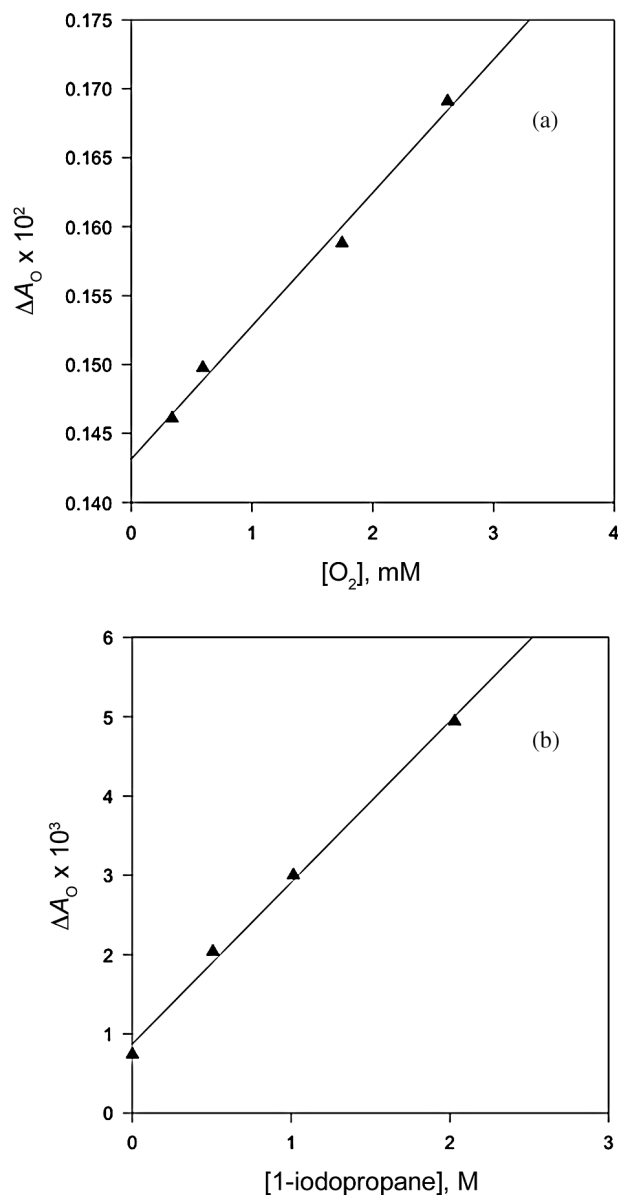$$H = k \times \alpha \times E_L \times (1 - 10^{-A}) \quad (1)$$

Fig. 5. Laser fluence dependence in laser flash photolysis experiments of ΔA_0 for the following toluene solutions: (; $\lambda^{obs} = 395$ nm) **2**, (Δ ; $\lambda^{obs} = 500$ nm) **7**, and ($\blacktriangle$; $\lambda^{obs} = 500$ nm) **8**

Fig. 4. Enhancement of S $\rightarrow$ T intersystem crossing in **8**: transient absorbance at zero time, ΔA_0, *vs* concentration of (a) oxygen and (b) 1-iodopropane (toluene solutions)

in which k is a proportionality constant involving geometrical parameters and thermoelastic properties of the solvent, and α is the fraction of absorbed energy dissipated as heat within the integration time (= prompt heat). In order to determine the α values for **7** and **8**, H *vs* E_L was monitored for N_2-saturated toluene solutions of **7**, **8**, and I_2, of various absorbances at λ^{exc}. The ratio of the slopes of the straight lines obtained for H/E_L plotted *vs* $(1 - 10^{-A})$ gave values of 0.78 ± 0.04 and 0.82 ± 0.06 for **7** and **8**, respectively. The lifetimes of the energy-storing species after excitation of **7** and **8**, *i.e.*, the triplet states, are much longer (77 and 36 μs, respectively; see Table 1) than the pressure-integration time of *ca*. 760 ns. This fact enables the use of the amplitude of the first LIOAS signal deflection and renders a more complex signal handling
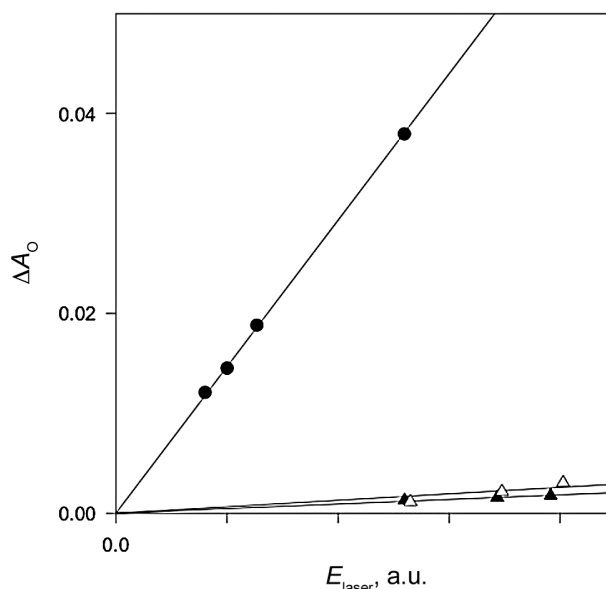
unnecessary [17]. Structural volume changes can be neglected in toluene.

The TD-DFT calculated maximum value of $\Delta\varepsilon = 100\,000$ $M^{-1}.cm^{-1}$ is located at around 430 nm (Fig. 3). One has to consider that in the experimental spectrum the triplet absorption overlaps with the singlet state depletion and the maximum is then shifted. The difference between the experimental and calculated maxima of ~70 nm (~0.3 eV), is in any case within the errors accepted for this type of calculations, *i.e.*, on the order of ~0.3–0.4 eV [18, 19].

The triplet energy at the O3LYP/6-311+G(2d)// O3LYP/6-311G(d) level calculated in toluene was $E_T = (96.0 \pm 10)$ $kJ.mol^{-1}$, in good agreement with the experimental value = (109 ± 3) $kJ.mol^{-1}$.

$O_2(^1\Delta_g)$ generation and quenching by 7 and 8

No $O_2(^1\Delta_g)$ phosphorescence was observed upon excitation of **7** and **8** in air-saturated toluene solutions. Thus, should $O_2(^1\Delta_g)$ be formed at all by quenching of triplet **7** and **8**, the quantum yield of generation would be $\Phi_\Delta < 10^{-3}$. Indeed, $O_2(^1\Delta_g)$ phosphorescence could be observed upon irradiation of air-saturated 1-iodopropane solutions of **7** ($A^{650} = 0.33$). The $O_2(^1\Delta_g)$ decay lifetime was 8.3 μs. No signal was observed from N_2-saturated 1-iodopropane solutions of **7**.

The values for the quenching constants of $O_2(^1\Delta_g)$ by **7** and **8**, k_q^Δ, were determined by time-resolved NIR experiments. $O_2(^1\Delta_g)$ was generated by energy transfer from triplet ZnTPP (excited at 532 nm where **7** and **8** have almost no absorption, Fig. 1, see Experimental section) to ground-state oxygen in the presence of **7** and **8**. The linear Stern-Volmer plots (not shown) yielded $k_q^\Delta = (2 \pm 1) \times 10^9$ $M^{-1}.s^{-1}$ and $(5 \pm 2) \times 10^9$ $M^{-1}.s^{-1}$, respectively. All quenching constants are compiled in Table 2.

Table 2. Quenching rate constants in toluene at room temperature

Quenched species	Quencher	k_q /(10^9 M^{-1}.s^{-1}) [a]
triplet **2**	**7**	0.8[b]
triplet **2**	**8**	1.0
triplet **7**	$O_2(^3\Sigma_g^-)$	0.41 ± 0.02
triplet **8**	$O_2(^3\Sigma_g^-)$	0.25 ± 0.02[b]
triplet **8**	1-iodopropane	0.26 ± 0.6
$O_2(^1\Delta_g)$	**7**	2 ± 1
$O_2(^1\Delta_g)$	**8**	5 ± 2

[a] A more explicit nomenclature differentiates the individual rate constants in the text. [b] Determined from only two quencher concentrations.

DISCUSSION

The photophysical properties of **7** and **8** are very similar. Similar to other porphycenes and expanded tetrapyrroles, also in this case the alkyl substituents do not affect the chromophoric properties [9].

In our earlier studies the triplet energies of some extended (22π and 26π) prophyrinoids have been found to lie below E_Δ [8]. As a consequence, they quench $O_2(^1\Delta_g)$ by irreversible energy transfer. The situation with the 22π porphyrinoids **7** and **8** is different. They quench $O_2(^1\Delta_g)$, generated by sensitization with ZnTPP, at lower than diffusion-controlled rates (*i.e.*, at $k_q < 3 \times 10^{10}$ M^{-1}.s^{-1} [20], see Table 2). Therefore, exothermic quenching of $O_2(^1\Delta_g)$ by **7** and **8** cannot be responsible for the energy transfer process observed.

Furthermore, the decays of both triplet **7** and **8** are monoexponential even in the presence of oxygen, which rules out the possibility of a reversible energy transfer between the triplet states of the porphyrinoids and ground state oxygen. These findings suggest that E_T for both compounds should be at least some 12 kJ.mol^{-1} higher than E_Δ (94.4 kJ.mol^{-1}), *i.e.*, $E_T \geq 106$ kJ.mol^{-1}. The calculated value of $E_T = (96.0 \pm 10)$ kJ.mol^{-1} supports these results.

The term $E^{exc} \times (1 - \alpha)$ of the energy balance Equation (2) [where E^{exc} is the excitation energy per mole of photons, α the prompt heat (*vide supra*), E_f the mean fluorescence energy, and E_T the triplet energy] affords 40.5 and 33.1 kJ.mol^{-1} for **7** and **8**, respectively. Since the energy stored in the triplet state, $\Phi_T^0 \times E_T$, should be negligible with respect to the fluorescence term (*vide supra* for E_T and Φ_T^0 for **7** and **8**), Equation 3 suffices for the determination of Φ_f.

$$E^{exc} \times (1 - \alpha) = \Phi_f \times E_f + \Phi_T^0 \times E_T \quad (2)$$

$$E^{exc} \times (1 - \alpha) \approx \Phi_f \times E_f \quad (3)$$

The values obtained in this way are $\Phi_f = (0.30 \pm 0.05)$ for **7** and $\Phi_f = (0.25 \pm 0.05)$ for **8**. The ratio Φ_f (**7**)/Φ_f (**8**) = 1.2 is in excellent agreement with the ratio of the emission areas (1.21, *vide supra*). We remark that, although the emission spectra are nicely obtained,

it is not trivial to obtain the values of Φ_f by the usual comparative method with emission standards, since in the far-red region of the spectrum no such standards are available. In fact, these extended tetrapyrroles may be used as far-red standards since we have now determined their Φ_f values with relatively high accuracy by LIOAS.

The low triplet yield of 0.02 for both compounds (Table 1) and the low S_Δ (=Φ_Δ/Φ_T) value, presumed to be as low as that observed previously for another 22π porphyrinoid (**6**) [8], preclude the observation of $O_2(^1\Delta_g)$ phosphorescence in toluene. However, $O_2(^1\Delta_g)$ phosphorescence is indeed observed upon irradiation of **7** and **8** in 1-iodopropane solutions. This result confirms that $E_T > E_\Delta$, since the heavy atom effect, which increases the triplet yields in this solvent, should not affect the value of the triplet energy.

The quenching of triplet **2** ($E_T = 124$ kJ.mol^{-1}) [14] by **7** and **8** is clearly slower than diffusion controlled (Table 2). Yet, the decay of triplet **2** in the presence of either **7** or **8** is monoexponential. The energy transfer should therefore be irreversible, and the triplet energy of both **7** and **8** should be at least 12 kJ.mol^{-1} lower than that of **2**, *i.e.*, 106.4 kJ.mol^{-1} ≤ E_T ≤ 112 kJ.mol^{-1} for both porphyrinoids. Similar relatively low k_q values have been reported also for the quenching of the triplet state of one 22π porphyrinoid (**6**) by the ground state of another one (**4**) [8]. The data indicate a steric hindrance for the triplet energy transfer as has been reported in the past [21].

EXPERIMENTAL

Toluene, 1-iodopropane and bromobenzene were spectroscopic grade (Merck, Uvasol). The laser dyes were from Radiant Dyes Chemie. Zinc(II) tetraphenylporphyrin (ZnTPP, from Aldrich) was purified by a method adopted from that described for tetraphenylporphyrin [22].

Synthesis and characterization

Compounds **7** and **8** were synthesized and characterized by Dietrich [6]. A brief description follows. The synthesis of **7** and **8** were performed through reductive coupling [23] of 5-formyl-5′-(2-formylvinyl)-4,4′-di-n-propyl-2,2′-bipyrrole, and 5-formyl-5′-(2-formylvinyl)-4,4′-di-t-butyl-2,2′-bipyrrole, respectively. These asymmetric 5-formyl-5′-(2-formylvinyl)-4,4′-di-alkyl-2,2′-bipyrroles can be obtained in one reaction using a sequence of a vinylogeous Vilsmeier formylation [24] and a Vilsmeier formylation.

Compound 7. Synthesis of 5-formyl-5′-(2-formyl-vinyl)-4,4′-di-n-propyl-2,2′-bipyrrole (precursor of 7). A solution of 3.8 g (25 mmol; 2.3 mL) phosphor(V)-oxidtrichloride in 250 mL CH$_2$Cl$_2$ was added drop by drop to a solution of 5.4 g (25 mmol) 4,4′-di-n-propyl-2,2′-bipyrrole [25] and 2.5 g (25 mmol; 2.6 mL) 3-(*N,N*-dimethylamino)acrolein in 500 mL CH$_2$Cl$_2$ under an Ar-atmosphere at -20 °C. In a second reaction step

45.7 g (625 mmol; 48 mL) N,N-dimethylformamide and subsequently 19.2 g (125 mmol; 11.7 mL) phosphor(V)-oxidtrichloride dissolved in 250 mL CH_2Cl_2 were added. Saponification of the bisiminium salt with 1 L of water and 500 mL 8% sodium hydroxide led to 5-formyl-5′-(2-formylvinyl)-4,4′-di-n-propyl-2,2′-bipyrrole (98% yield). After several recrystallizations from (1:1) ethanol/CH_2Cl_2 golden needles of 5-formyl-5′-(2-formylvinyl)-4,4′-di-n-propyl-2,2′-bipyrrole, which decomposed at 222 °C, were obtained. A slurry of 5.5 g (84 mmol) activated zinc and 416 mg (4.2 mmol) copper(I) chloride in 900 mL tetrahydrofuran was treated dropwise with 4.6 mL (42 mmol) titanium tetrachloride under argon. A hot solution of 1.2 g (4 mmol) 5-formyl-5′-(2-formylvinyl)-4,4′-di-n-propyl-2,2′-bipyrrole in 300 mL tetrahydrofuran was slowly dropped (within a period of 20 min) into the reaction mixture. After addition of 150 mL of a dilute solution of ammonia and 200 mL dichloromethane the initially red solution turned green. The separation of **7** was performed by chromatography using CH_2Cl_2 on neutral aluminum oxide. At the beginning small amounts of a by-product were obtained. Then, **7** was eluted with a saturated ammonia solution in CH_2Cl_2. Crystallization from benzene yielded cubic crystals of **7** with a 7% yield. The crystals decomposed at 215 °C. Compound **7** is soluble in chloroform, methylene chloride, and tetrahydrofuran, and moderately in aromatic hydrocarbons. It is practically insoluble in aliphatic hydrocarbons, diethylether, alcohols, acetonitrile, and dimethylsulfoxide. Both in solution and as a powder compound **7** was found to be stable. ^{1}H NMR (300 MHz, $CDCl_3$): δ, ppm 10.82 (d, J = 13.5 Hz, 2H), 10.39 (m, J = 13.7 Hz, 2H), 9.68 (d, J = 9.9 Hz, 2H), 9.50 (s, 2H), 9.33 (s, 2H), 4.34 (t, J = 7.6 Hz, 4H), 4.06 (t, J = 7.6 Hz, 4H), 2.64 (sext., J = 7.3 Hz, 4H), 2.49 (sext., J = 7.3 Hz, 4H), 1.52 (t, 6H), 1.44 (t, 6H), -7.07 (t, 2H). ^{1}H NMR (300 MHz, $CDCl_3/Al_2O_3$): δ, ppm 11.05 (d, J = 13.8 Hz, 2H), 10.63 (m, J = 13.4 Hz, 2H), 9.93 (d, J = 9.9 Hz, 2H), 9.68 (s, 2H), 9.47 (s, 2H), 4.40 (t, J = 7.6 Hz, 4H), 4.15 (t, J = 7.6 Hz, 4H), 2.66 (sext., J = 7.3 Hz, 4H), 2.54 (sext., J = 7.3 Hz, 4H), 1.51 (t, 6H), 1.46 (t, 6H), -4.13 (br s, 4H), -7.00 (t, 2H). MS (E/I, 70 eV): m/z 532 (31%), 530 (100%, [M][+.]), 501 (24%), 487 (31%), 472 (2%), 458 (5%), 443 (2%), 429 (5%), 414 (2%), 400 (2%), 386 (2%), 266 (4%), 265 (13%, [M][2+]), 250.5 (2%), 243.5 (1%), 236 (6%), 229 (4%), 221.5 (3%), 214.5 (2%), 207 (3%), 200 (3%), 193 (2%). High resolution MS (EI): m/z 530.3409 (calcd. for $C_{36}H_{42}N_4$ [M][+.] 530.3409). Elemental analysis C 78.61, H 8.21, N 10.10 (calcd. for $C_{36}H_{42}N_4 \cdot H_2O$ (548.778 g/mol) C 78.89, H 8.08, N 10.21).

Compound 8. Compound **8** was prepared by a McMurry coupling of 5-formyl-5′-(2-formylvinyl)-4,4′-di-t-butyl-2,2′-bipyrrole following a similar procedure as that employed for the synthesis of **7**. 5-formyl-5′-(2-formylvinyl)-4,4′-di-t-butyl-2,2′-bipyrrole can be obtained from 4,4′-di-t-butyl-2,2′-bipyrrole [26] following the procedure described above. Chromatographic purification

with methylene chloride on aluminum oxide yielded compound **8** in the green third fraction. This compound was eluted with ammonia and, after recrystallization with 1:1 methylene chloride: methanol, blue diamond-shaped crystals of **8**, which slowly decomposed at 280 °C, were obtained with a 10% yield. The solubility of compound **8** in various solvents is higher than that of **7**. Compound **8** is very soluble in chlorinated and aromatic hydrocarbons, as well as in diethylether. It is also relatively soluble in aliphatic hydrocarbons and slightly soluble in alcohols and acetonitrile. ^{1}H NMR (300 MHz, $CDCl_3$): δ, ppm 11.16 (d, J = 13.5 Hz, 2H), 10.47 (m, J = 13.4 Hz, 2H), 10.20 (d, J = 10.2 Hz, 2H), 9.51 (s, 2H), 9.43 (s, 2H), 2.46 (s, 18H), 2.38 (s, 18H), -2.62 (br. s, > 4H), -6.14 (t, 2H). ^{1}H-NMR (300 MHz, $CDCl_3/Al_2O_3$): δ, ppm 11.15 (d, J = 13.5 Hz, 2H), 10.46 (m, J = 13.5 Hz, 2H), 10.20 (d, J = 10.2 Hz, 2H), 9.50 (s, 2H), 9.41 (s, 2H), 2.46 (s, 18H), 2.38 (s, 18H), -3.58 (br s, 4H), -6.38 (t, 2H). MS (E/I, 70 eV): m/z 601 (2%), 588 (22%), 587 (50%), 586 (100%, [M][+.]), 571 (22%), 531 (6%), 530 (17%), 529 (39%), 515 (7%), 514 (10%), 499 (14%), 473 (6%), 472 (6%), 457 (8%), 442 (4%), 415 (2%), 294 (7%), 293.5 (5%), 293 (27% M[2+]), 292 (50%), 285.5 (6%), 278 (19%), 249.5 (4%). High resolution MS (EI): m/z 586.4035 (calcd. for $C_{40}H_{50}N_4$ [M][+.] 586.4035). Elemental analysis C 71.22, H 7.56, N 7.76 (calcd. for $C_{40}H_{50}N_4 \cdot H_2O$ (604.887 g.mol^{−1}) C 71.67, H 8.02, N 7.96).

Optical spectroscopic methods

Degassed solutions were prepared by five freeze-pump ($< 10^{-1}$ Pa)-thaw cycles. A computer-controlled Shimadzu UV-2102 spectrophotometer was employed for the absorption measurements.

Steady-state NIR luminescence

Steady-state NIR luminescence was measured with a home-built NIR emission spectrophotometer. The excitation light from a 2500-W Xe lamp was filtered through 3 cm of water, two KG-5 filters, and a 651 nm band-pass filter (Schott, Mainz). A cut-off filter (700 nm) was placed between the monochromator (with a grating blazed at 1 m) and the Ge detector. The emission spectra were recorded at room temperature. The absorbances of the solutions of **7** and **8** at the excitation wavelength (λ^{exc} = 651 nm) were 0.171 ± 0.001.

Singlet-excited state lifetimes

Singlet-excited state lifetimes, τ_S, were measured in air-saturated solutions with a single-photon-counting fluorimeter. The details of the instrumental set-up and the mathematical algorithm for the data handling have been published elsewhere [27, 28]. The excitation and emission wavelengths were 354 and 848 nm, respectively, for both compounds. Absorbances at the excitation wavelength were A_{354} = 0.063 and 0.053 for the solutions of **7** and **8**, respectively.

Triplet measurements by flash photolysis

Triplet measurements by flash photolysis were carried out with an improved version of the system described previously [29]. For excitation, a dye laser (DCM, λ = 650 nm) was pumped with the second harmonic of a Q-switched Nd:YAG laser (System 2000, J.K. Lasers; pulse width 15 ns).

The comparative method [13] was employed for the determination of the S → T intersystem crossing quantum yield in the absence of oxygen (Φ^0_T). The values of the product $\Delta\varepsilon \, \Phi^0_T$ in degassed toluene solutions were obtained with $\Delta\varepsilon$ the difference in molar absorption coefficient at the observation wavelength (λ^{obs}) for the respective transient absorbance, after excitation with a laser pulse, and assigned in these experiments to the respective triplet state plus the ground-state depletion. The dependence of the transient absorbance (extrapolated to zero time, ΔA_0) on the laser fluence was determined at λ^{obs} = 500 (assigned to the triplet absorption without singlet interference for **7** and **8,** see Figs 1 and 2) and 395 nm (for the reference compound **2**, for which the product $\Delta\varepsilon(395) \times \Phi^0_T = 8400$ $M^{-1}.cm^{-1}$) [14]. The absorbance of sample and reference solutions was matched at the excitation wavelength (A_{650} = 0.500).

The effect of molecular ground state oxygen on the triplet state kinetics was analyzed by monitoring the triplet decays of **7** and **8** in toluene as a function of O_2 concentration. For this purpose, O_2/N_2 mixtures were bubbled into the solution, and the O_2 concentration was calculated by using Henry's law and an O_2 concentration of 2.1 mM in air-saturated toluene [30].

The quantum yields of triplet **7** and **8**, produced at λ^{exc} = 650 nm in degassed toluene solutions of A_{650} ~ 0.27 with 0-2.03 M 1-iodopropane, were estimated from the values of ΔA_0.

Time-resolved NIR luminescence

The $O_2(^1\Delta_g)$ emission was measured with the set-up previously described [31]. In order to check the $O_2(^1\Delta_g)$ generation upon excitation of **7** and **8**, air-saturated toluene and 1-iodopropane solutions of these compounds were irradiated with λ^{exc} = 650 nm at various laser fluences. In view of the relatively strong fluorescence of the compounds in the spectral region where $O_2(^1\Delta_g)$ emits, a narrow band-pass filter of (1270 ± 10) nm and low laser fluences were employed in order to avoid detector ringing effects. Such effects would cause spurious signals which cannot be fitted by exponential functions. The rate constants for the quenching of $O_2(^1\Delta_g)$ by **7** (in concentrations of 0.68–15 μM) and **8** (0.17–34 μM) in toluene were determined in conventional Stern–Volmer experiments [32] with ZnTPP (λ^{exc} = 532 nm, A_{532} = 0.460) as a sensitizer in air-saturated solutions. The laser fluence was < 0.2 mJ.cm^{-1}.

Laser-induced optoacoustic spectroscopy (LIOAS)

N_2-saturated toluene solutions, with A_{650} = 0.05–0.16 for **7**, **8** and I_2 (as a calorimetric reference [15]), were excited by a dye laser (λ^{exc} = 650 nm). The pressure integration time [16] was 760 ns, and the laser fluence was kept < 15 μJ per pulse.

Time-dependent density functional theory (TD-DFT) calculations

Absorption spectra were calculated employing the hybrid functional O3LYP/6-311+G(d) [33] with the CPCM model in toluene (relative permittivity = 2.37419).

The TD-DFT calculations do not account for vibrational broadening. Therefore, to compare with experimental results spectra were obtained by representing each electronic transition with Gaussian shape functions centered at the calculated band maxima. The whole spectra were then obtained simply by adding over all derived transitions. The value of the width at half maximum, ΔE = 0.22 eV, was employed to reproduce the experimental absorption coefficient of the Soret band of compound **7** at 445 nm ($\varepsilon/M^{-1}.cm^{-1}$ = 179 700). The calculated molar absorption coefficient at 445 nm was $\varepsilon/M^{-1}.cm^{-1}$ = 177 000. The T-T absorption spectrum was calculated with the same ΔE value and finally the values of $\Delta\varepsilon_{T\text{-}T}$ were obtained as the absorption spectra of the triplet (Fig. 3).

CONCLUSION

A combination of near IR steady-state and time-resolved emission, laser-induced optoacoustic spectroscopy, as well as triplet and $O_2(^1\Delta_g)$ quenching experiments has allowed the calculation of the photophysical properties of the 22π porphyrinoids **7** and **8**. The TD-DFT calculations afforded results in agreement with the experimental data. These compounds have very similar photophysical properties, they are highly fluorescent in an aromatic organic solvent such as toluene but produce very inefficiently triplet states. Consequently, in spite of having a triplet energy higher than that of $O_2(^1\Delta_g)$, the production of this species is not at all efficient. The values of the fluorescence quantum yields for **7** and **8** are similar to the value determined for the parent compounds **1** and **2**. However, the value of Φ_f decreases with an increase in number of C atoms introduced between the adjacent pyrrolic rings of porphycene (compounds **3**, **4**, and **6**) [8]. The flexibility introduced by the expansion of the ring in both directions increases in every case the internal conversion and decreases the triplet yields of the porphyrinoid compounds (*cf.* Table 1 as well as Table 1 in Mártire *et al.* [8]).

Acknowledgements

REFERENCE

1. For leading references on the porphycenes, see Vogel E. *Pure Appl. Chem.* 1996; **68**: 1355–1360; Vogel E, Bröring M, Fink J, Rosen D, Schmickler H, Lex J, Chan KWK, Wu YD, Plattner DA, Nende M and Houk KN. *Angew. Chem. Int. Ed. Engl.* 1995; **34**: 2511–2514; Wu YD, Chan KWK, Yip CP, Vogel E, Plattner DA and Houk KN. *J. Org. Chem.* 1997; **62**: 9240–9250; Vogel E. *Chemicke Listy* 1999; **93**: 767–773; and the more recent review Sánchez-García D and Sessler JL. *Chem. Soc. Rev.* 2008; **37**: 215–232.

2. Jux N, Koch P, Schmickler H, Lex J and Vogel E. *Angew. Chem. Int. Ed. Engl.* 1990; **29**: 1385–1387.

3. Substitution with ethyl groups or higher alkyls provide for better solubility.

4. For the expansion to a 26 porphyrinoid see [8].

5. Vogel E, Jux N, Rodriguez-Val E, Lex J and Schmickler H. *Angew. Chem. Int. Ed. Engl.* 1990; **29**: 1387–1390.

6. Dietrich H-J. Ph.D. Thesis, Universität Köln (1994).

7. a) Guardiano M, Biolo R, Jori G and Schaffner K. *Cancer Lett.* 1989; **44**: 1–6. b) Milanesi C, Biolo R, Jori G, Schaffner K and Vogel E. *Lasers Med. Sci.* 1991; **6**: 437–442. c) Schaffner K, Vogel E and Jori G. In *Biologic Effects of Light 1993*, Jung EG and Holick MF. (Eds.) Walter de Gruyter: Berlin, 1994; pp 312–321. d) Toledano H, Edrei R and Kimel S. *J. Photochem. Photobiol. B: Biol.* 1998; **42**: 20–27. e) For a more recent review regarding porphycenes as photodynamic agents see: Stockert JC, Cañete M, Juarranz A, Villanueva A, Horobin RW, Rorrell JI, Teixedó J and Nonell S. *Current. Med. Chem.* 2007; **14**: 997–1026.

8. Mártire DO, Jux N, Aramendía PF, Negri RM, Lex J, Braslavsky SE, Schaffner K and Vogel E. *J. Am. Chem. Soc.* 1992; **114**: 9969–9978.

9. Braslavsky SE, Müller M, Mártire DO, Pörting S, Bertolotti SG, Chakravorti S, Koç-Weier G, Knipp B and Schaffner K. *J. Photochem. Photobiol. B: Biol.* 1997; **40**: 191–198; Errata, *ibid* 1998; **42**: 79.

10. Rihter, BD, Kenney ME, Ford WE and Rodgers MAJ. *J. Am. Chem. Soc.* 1990; **112**: 8064–8070.

11. a) Firey PA, Ford WE, Sounik JR, Kenney ME and Rodgers MAJ. *J. Am. Chem. Soc.* 1988; **110**: 7626–7630. b) Ford WE, Rihter BD and Rodgers MAJ. *J. Am. Chem. Soc.* 1989; **111**: 2362–2363.

12. Kasha M. In *Singlet O₂*, Vol. I, Frimer AA. (Ed.) CRC Press: Boca Raton, 1988; pp 1–12.

13. Bensasson RV, Goldschmidt CR, Land EJ and Truscott TG. *Photochem. Photobiol.* 1978; **28**: 277–281.

14. Nonell S, Aramendía PF, Heihoff K, Negri RM and Braslavsky SE. *J. Phys. Chem.* 1990; **94**: 5879–5883.

15. Tam AC, Patel CKN and Kerl RJ. *Opt. Lett.* 1979; **4**: 81.

16. a) Braslavsky SE and Heibel GE. *Chem. Rev.* 1992; **92**: 1381–1410. b) Gensch T and Viappiani C. *Photochem. Photobiol. Sci.* 2003; **2**: 699–721.

17. Habib Jiwan JL, Wegewijs B, Indelli MT, Scandola F and Braslavsky SE. *Recl. Trav. Chim. Pays-Bas* 1995; **114**: 542–549.

18. Grime S. in *Reviews in Computational Chemistry*, Vol. 20, Ch. 3, Lipkowitz KB, Larter R and Cundari TR. (Eds.) Wiley-VCH, John Wiley & Sons, Inc.: New York, 2004.

19. Zhao Y and Truhlar DG. *Acc. Chem. Res.* 2008; **41**: 157–167.

20. Ware WR. *J. Phys. Chem.* 1962; **66**: 455–458.

21. Scaiano JC, Leigh WJ, Meador MA and Wagner PJ. *J. Am. Chem. Soc.* 1985; **107**: 5806–5807.

22. Rousseau K and Dolphin D. *Tetrahedron Lett.* 1974; **48**: 4251–4254.

23. a) McMurry JE. *Chem. Rev.* 1989; **89**:1513–1524. b) Lenoir D. *Synthesis-Stuttgart* 1989; 883–897. c) Dams R, Malinowski M, Westdorp I and Geise HY. *J. Org. Chem.* 1982; **47**: 248–259. d) McMurry JE and Fleming MP. *J. Am. Chem. Soc.* 1974; **96**: 4708–4709.

24. Ullrich FW and Breitmaier E. *Synthesis-Stuttgart* 1983; 641–645.

25. a) Vogel E, Balci M, Pramod K, Koch P, Lex J and Ermer O, *Angew. Chem. Int. Ed.* 1987; **26**: 928–931. b) Vogel E, Köcher M, Schmickler H and Lex J. *Isr. J. Chem.* 1989; **29**: 257–266.

26. Donnerstag D. Ph.D. Thesis, Universität Köln (1993), Hellwig Y. Ph.D. Thesis, Universität Köln (1994).

27. Matthews JI, Braslavsky SE and Camilleri P. *Photochem. Photobiol.* 1980; **32**: 733–738.

28. Wendler J, Holzwarth AR, Braslavsky SE and Schaffner K. *Biochim. Biophys. Acta* 1984; **786**: 213–221.

29. a) Aramendía PF, Ruzsicka BP, Braslavsky SE and Schaffner K. *Biochemistry* 1987; **26**: 1418–1422. b) Ruzsicka BP, Braslavsky SE and Schaffner K. *Photochem. Photobiol.* 1985; **41**: 681–688.

30. Murov SL. *Handbook of Photochemistry*, (2nd ed.) Dekker: New York, 1994; pp 292.

31. a) Martínez G, Bertolotti SG, Zimerman OE, Mártire DO, Braslavsky SE and García NA. *J. Photochem. Photobiol. B: Biology* 1993; **17**: 247–255. b) Yruela I, Churio MS, Gensch T, Braslavsky SE and Holzwarth AR. *J. Phys. Chem.* 1994; **98**: 12789–12795.

32. Mártire DO, Braslavsky SE and García NA. *J. Photochem. Photobiol. A: Chem.* 1991; **61**: 113–124.

33. Dell'Arciprete ML, Cobos CJ, Furlong JP, Mártire DO and Gonzalez MC. *Chem Phys Chem* 2007; **8**: 2498–2505.